Analytical and Bioanalytical Chemistry (2019) 411:629–637
https://doi.org/10.1007/s00216-018-1477-9

RESEARCH PAPER

Complementarity of molecular and elemental mass spectrometric imaging of Gadovist™ in mouse tissues

Sabrina Trog[1] · Ahmed H. El-Khatib[1,2] · Sebastian Beck[1] · Marcus R. Makowski[3] · Norbert Jakubowski[2] · Michael W. Linscheid[1]

Received: 27 September 2018 / Revised: 30 October 2018 / Accepted: 5 November 2018 / Published online: 20 November 2018

Abstract

Drug biodistribution analyses can be considered a key issue in pharmaceutical discovery and development. Here, mass spectrometric imaging can be employed as a powerful tool to investigate distributions of drug compounds in biologically and medically relevant tissue sections. Both matrix-assisted laser desorption ionization–mass spectrometric imaging as molecular method and laser ablation inductively coupled plasma–mass spectrometric imaging as elemental detection method were applied to determine drug distributions in tissue thin sections. Several mouse organs including the heart, kidney, liver, and brain were analyzed with regard to distribution of Gadovist™, a gadolinium-based contrast agent already approved for clinical investigation. This work demonstrated the successful detection and localization of Gadovist™ in several organs. Furthermore, the results gave evidence that gadolinium-based contrast agents in general can be well analyzed by mass spectrometric imaging methods. In conclusion, the combined application of molecular and elemental mass spectrometry could complement each other and thus confirm analytical results or provide additional information.

Keywords Matrix-assisted laser desorption ionization–mass spectrometry imaging (MALDI-MSI) · Laser ablation inductively coupled plasma–mass spectrometry imaging (LA-ICP-MSI) · Gadolinium-based contrast agents (GBCAs)

Introduction

Magnetic resonance imaging (MRI) is a powerful imaging technique for the non-invasive examination of human anatomy, physiology, and pathophysiology. Furthermore, with the introduction of contrast agents (CAs), the applications of diagnostic MRI have increased further. Various types of CAs have been designed and further developed; however, gadolinium-based contrast agents (GBCAs) are currently the most frequently used MRI CAs [1].

Gd^{3+} salts cannot be applied in the ionic form due to their toxicity. As a consequence, ligands have been designed that complex the toxic metal ion. Here, acyclic and macrocyclic polyaminocarboxylates, specifically diethylenetriaminepentaacetic acid (DTPA) or 1,4,7,10-tetraazacyclododecane-N,N′,N″,N‴-tetraacetic acid (DOTA), as well as other derivatives are frequently applied in a variety of available GBCAs [2]. The open-chain DTPA and the macrocyclic DOTA are chelating agents that form high stability complexes with a variety of metal ions, resulting in complexes that meet the strict requirements for intravenously administered drugs. Thermodynamic stability and kinetic inertness are among the most important features, and GBCAs with a cyclic chelate are considered to be especially safe and well tolerated [3]. Nowadays, about 30% of all clinical MRI scans utilize application of these GBCAs [4]. Once administered, the extracellular agents

Published in the topical collection *Elemental and Molecular Imaging by LA-ICP-MS* with guest editor Beatriz Fernández García.

Sabrina Trog and Ahmed H. El-Khatib contributed equally to this work.

Electronic supplementary material The online version of this article (https://doi.org/10.1007/s00216-018-1477-9) contains supplementary material, which is available to authorized users.

✉ Sebastian Beck
s.beck@chemie.hu-berlin.de

[1] Department of Chemistry, Humboldt-Universität zu Berlin, Brook-Taylor-Str. 2, 12489 Berlin, Germany

[2] Bundesanstalt für Materialforschung und –prüfung, Richard-Willstätter-Str. 11, 12489 Berlin, Germany

[3] Department of Radiology, Charité – Universitätsmedizin Berlin, Charitéplatz 1, 10117 Berlin, Germany

distribute quickly through the intravascular and interstitial (space between cells) fluid compartments. In general, the terminal half-life for blood elimination is about 1.5 h in a healthy human individual. These agents are cleared almost exclusively renally by glomerular filtration [1, 3, 5].

The method of choice for precise determination of distributions of GBCAs in various tissue samples appears to be laser ablation inductively coupled plasma–mass spectrometric imaging (LA-ICP-MSI). The reasons are obvious: LA-ICP-MSI offers highly sensitive, very accurate, multi-elemental analyses of trace and ultra-trace elements in a large linear and dynamic range. Postmortem imaging of gadolinium distributions was performed in a mouse tumor model after administration of PEGylated gadolinium liposomal nanoparticles. Kamaly et al. reported that Gd was prevalent in regions of higher vascularity when correlated to histology. The presence of Gd in kidneys was also confirmed, suggesting that the PEGylated gadolinium liposomal nanoparticles were processed by the renal excretion pathway [6]. LA-ICP-MSI of histological sections was correlated with in vivo MRI by Pugh and coworkers, where LA-ICP-MSI had been used to map the spatial distribution of GBCAs in rat and pig brains. Gadolinium uptake by aquatic and terrestrial organisms and its distribution was determined by Lingott et al. using LA-ICP-MSI [7].

However, LA-ICP-MSI cannot provide any information about molecular structures of the analytes. Thus, matrix-assisted laser desorption/ionization–mass spectrometry (MALDI-MS) is a very promising tool not only to analyze the distributions of GBCAs, but also to determine the chemical form of the Gd-based analyte. Nevertheless, only two studies have investigated the analysis of GBCAs in biological tissue sections applying MALDI-MSI. Acquadro and coworkers described the analysis of mouse livers after administration of GBCAs, where the identity of the CA was confirmed by fragmentation experiments. Later, a second study performed spatially resolved quantification of different GBCAs in tissues by MALDI-MSI after in vivo MRI. In this case, MALDI-MSI was able to corroborate the MRI signals and enabled in situ quantification of the GBCAs with high spatial resolution [8]. These publications reflect the potential advantages of MSI techniques when studying GBCAs.

In the current work, MALDI-MSI and LA-ICP-MSI have been performed to investigate the distribution of Gadovist™ (Gd(BT-DO3A)), a DOTA-based GBCA (Fig. 1) in mouse organs.

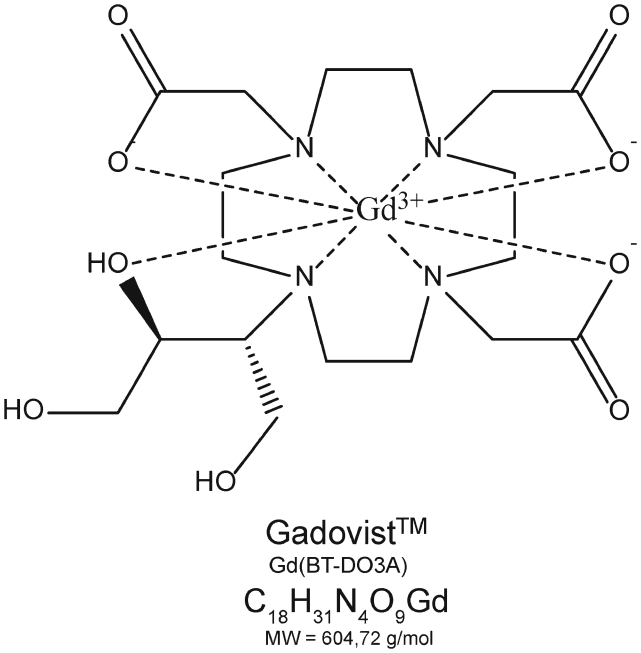

Fig. 1 Molecular structure of Gadovist™, sum formula and molecular weight

Materials and methods

Drug administration

Gadovist™ was administered into the heart in a quantity of two times 0.2 mmol Gd kg^{-1} from a 1 mmol mL^{-1} solution. Both injections were carried out quickly in a row. For heart, kidney, and liver investigations, the mouse was sacrificed 3 min after CA administration; the organs were removed and immediately snap-frozen in liquid nitrogen. The brain was removed 4 days post CA injection.

Cryo-sectioning

The organs were stored in a freezer at − 80 °C until cryo-sectioning. The frozen tissues were placed onto the mounting plate that was cooled to − 60 °C. Sections with a thickness of 10 μm were cryo-sectioned using a commercial cryostat (Thermo Fisher Scientific, CryoStar NX50 or Leica Biosystems, CM3050 S), and thin sections were transferred onto Superfrost Plus slides (Thermo Fisher Scientific). Glass slides were kept at − 80 °C until further sample preparation.

Thin section preparation for mass spectrometry imaging

Prior to further preparations, samples were allowed to thaw in an evacuated glass desiccator with silica gel to avoid water condensation and preserve the spatial resolution of the CA. The tissue samples were dried completely for about 30 min. The thin sections were covered with the matrix using a double action A470 airbrush (Aztek) with a high flow 0.50 mm diameter nozzle and argon as nebulizer gas at 1.8 bar. Matrix application was performed in 15 or 30 coating cycles with 500 μL matrix solution each. The matrix consisted of 20 mg mL^{-1} DHB in ACN/H_2O 60:40 and 0.1% TFA. The

matrix was allowed to dry under the argon gas flow for 1 min before the next coating cycle started.

MALDI-MS and MALDI-MSI analysis

The experiments were performed using a MALDI Orbitrap XL™ mass spectrometer (Thermo Fisher Scientific) equipped with a standard nitrogen UV laser (337 nm). The laser spot size on tissue was about 75 μm in diameter, and the laser raster step size was 120 μm in both directions in all cases. All MALDI-MSI analyses were performed in the Orbitrap™ part of the instrument in positive ion mode, and the resolving power was set 60,000 in all cases. Mass selection for fragmentation was performed in the linear ion trap with a collision energy of 35.0% using an isolation window of $\Delta m/z = 2$.

ICP-MS and LA-ICP-MSI analysis

A double-focusing sector field-based ICP mass spectrometer (ELEMENT XR™, Thermo Fisher Scientific) was used for the analyses. The ICP was tuned each day for maximum signal intensity and stability using tune-up solution ELEMENT including 1 μg L^{-1} of Ba, B, Co, Fe, Ga, In, K, Li, Lu, Na, Rh, Sc, Tl, U, and Y in 5.0% HNO_3 (Thermo Fisher Scientific). The instrument was operated in low-resolution mode ($R = 300$). For LA-ICP-MSI, a commercial laser ablation system (UP213, ESI) coupled to the ICP-MS system was used. The combined LA-ICP system was tuned on a daily basis for maximum signal intensity and stability using the standard reference material (SRM 612, NIST). The samples were printed with Ho-spiked ink using a modified commercial ink-jet printer (Canon iP4950) [9, 10].

For imaging experiments, a defined sample area was ablated line by line with a focused Nd:YAG laser beam. The Nd:YAG laser was operated at 213 nm. The laser energy and line scan overlapping were tuned for complete ablation of the tissue sample. The ablated material was transported by the carrier gas helium into the ICP torch. The detailed operating conditions for LA-ICP-MS measurements were as follows: RF power 900–1300 W, plasma gas 15 L min^{-1}, sample gas 1.3 L min^{-1}, auxiliary gas 0.8 L min^{-1}, number of passes 1. The LA system was operated with the following parameters: transport gas 0.8 L min^{-1}, laser fluence 3.92–4.15 L cm^{-2}, laser repetition rate 20 Hz, laser spot size 100 μm, scan speed 100 μm s^{-1}. ^{158}Gd was monitored as analyte, ^{165}Ho was used as internal standard, and ^{153}Eu was assessed for the general accumulation of lanthanides due to environmental exposure. Additionally, ^{31}P, ^{34}S, ^{57}Fe, ^{63}Cu, and ^{66}Zn were also monitored.

Results and discussion

Several possibilities of sample preparation and instrumental setups lead to successful results in MSI. However, each step needs to be adapted precisely to the respective kind of sample and characteristics of the analytes. In this work, the following methodology was applied whereas each individual step was optimized for a successful outcome of the experiment (Fig. 2).

MALDI-MS and MALDI-MSI

Different matrix substances were tested for MALDI analyses. Initially, standard spotting experiments were performed, applying different matrices at different concentrations (50 nmol–500 fmol per spot) of CA. Here, particular attention was given to the signal intensity of Gadovist™ and to possible spectral interferences of the analyte with matrix-derived signals. 2,5-Dihydroxybenzoic acid (DHB), α-cyano-4-hydroxycinnamic acid (CHCA), sinapinic acid (SA), 2′,5′-dihydroxyacetophenone (2,5-DHAP), niacin, and 3-hydroxypicolinic acid (3-HPA) were investigated. It was established that DHB as well as CHCA yielded best results concerning both points.

Subsequently, the solvent mixture for matrix application was optimized on microscope slides. Several mixtures of acetonitrile/water were tested for both DHB and CHCA, while in conclusion, 20 mg mL^{-1} DHB in acetonitrile/water 60:40 or 70:30 with 0.1% TFA was most suited. Application of DHB in these mixtures yielded small matrix crystals with a good homogeneous coverage, as verified by microscopic examination of the samples after matrix deposition. Higher contents of organic solvent resulted in larger crystals and were thus not used for MALDI-MSI experiments. The use of methanol rather than acetonitrile also yielded a largely unsuitable matrix deposition. The same was observed for CHCA in general, as here a rather thin and inhomogeneous deposition of matrix on the surfaces was detected (see Electronic Supplementary Material (ESM) Fig. S1).

Subsequently, Gadovist™ was spotted in various concentrations using DHB as matrix and analyzed to determine the concentration working range. In all cases, the Gd complex showed much lower intensities compared to the free chelate not carrying Gd^{3+}. This was in agreement with corresponding HPLC-MS experiments, where we also detected a higher response from the free chelates in comparison to the Gd-carrying CA (data not shown). The Gd-carrying complexes could be detected down to 1 pmol $spot^{-1}$ with a linear response up to at least 25 pmol $spot^{-1}$.

For MSI, three mice were administered in vivo with Gadovist™, which can be regarded as extracellular agent. Gadovist™ could be successfully detected by MALDI-MSI when applying the sample preparation methodology (Fig. 2; see ESM Fig. S2). However, a point which had to be considered was the normalization of MALDI-MSI results. Normalization

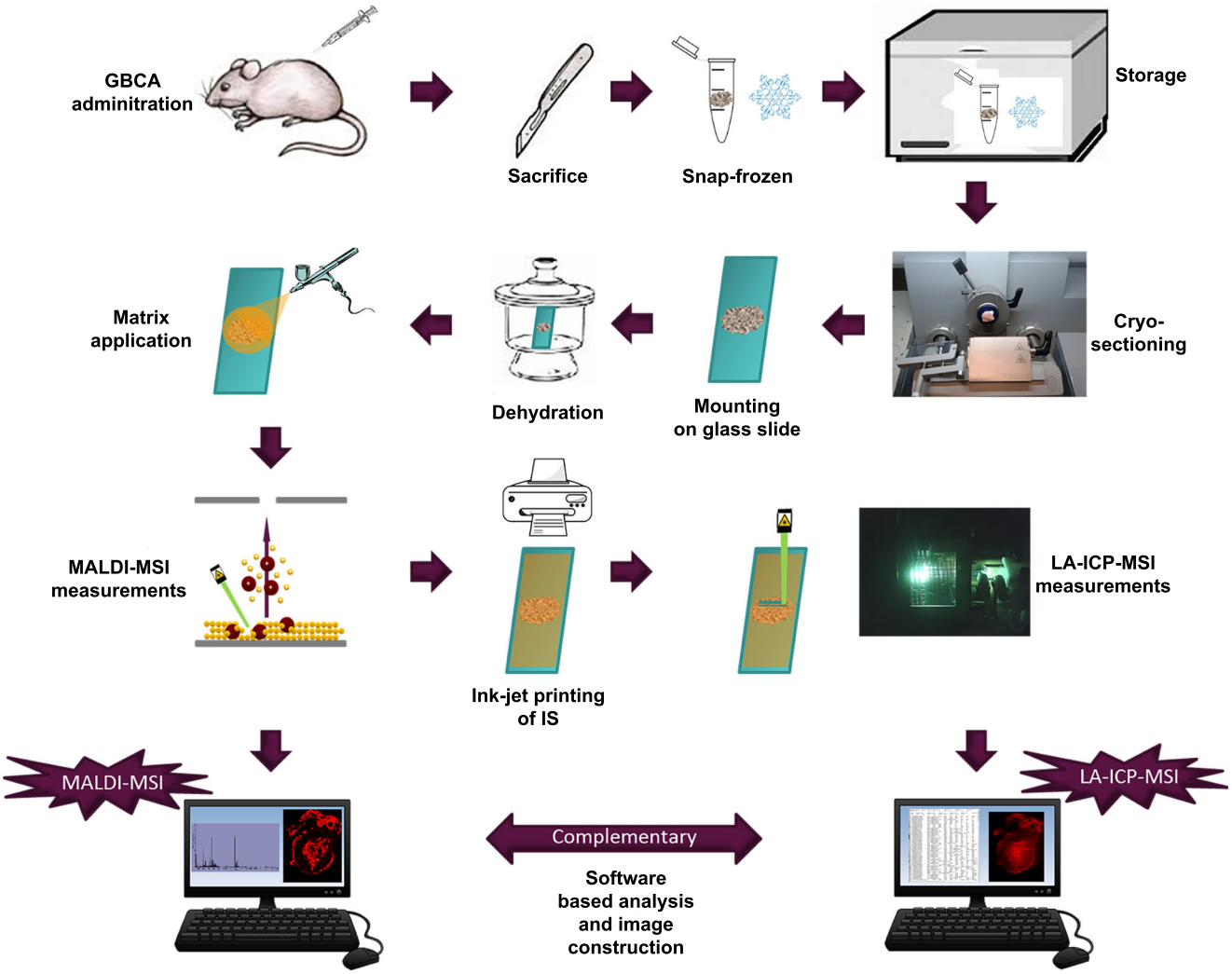

Fig. 2 Applied methodology in this work

is a requirement for the comparison of signal intensities of certain species within a tissue section. Instrumental fluctuations within long-term measurements result in drifts of signal intensities. This includes laser stability, matrix sublimation, extraction efficiency, ionization efficiency, ionization suppression, detection efficiency, multiple charge states, and ion stability [11]. We investigated two normalization approaches: firstly the normalization to the total ion current (TIC) and secondly the normalization to the DHB matrix signal *m/z* 273.039 ([2 DHB - 2 H_2O+H]$^+$, [$C_{14}H_9O_6$]$^+$). Comparing both normalization methods, the analyte distributions were generally similar. Normalization to the DHB matrix signal yielded higher signal rations in comparison to normalization to the TIC (see ESM Fig. S3). Thus, we decided to use *m/z* 273.039 as normalization signal. In order to ensure that the observed signals were correctly assigned to the analytes, the following was considered. The identification of the contrast agent signals was verified by the *m/z* signal itself using high-resolution MS data ($R = 60{,}000$). Moreover, control tissue sections (non-dosed tissues) did not exhibit signals related to the free ligand (BT-DO3A) at *m/z* 451.240 ([M+H]$^+$) or the GBCA (Gd (BT-DO3A)) at *m/z* 606.141 ([M+H]$^+$). Both also did not show any signals of potential Na^+ or K^+ adducts in non-dosed tissues. Additional CID fragmentation experiments were performed within dosed tissue sections. These MALDI-MS/MS spectra were identical to those of the pure compounds and confirmed that the observed *m/z* signals belonged to Gadovist™ and the free ligand. Furthermore, gadolinium possesses a unique isotopic pattern that also assisted in assigning corresponding signals (see ESM Fig. S4).

Gadovist™ could be detected and localized within distinct mouse tissue sections such as the heart, kidney, and liver by MALDI-MSI (Fig. 3b). These tissue sections belonged to sagittal sections from the center of the respective organ. Regarding heart tissue sections, the Gd complex [Gd (BT-DO3A)+H]$^+$ could be detected all over the tissue sections with distinct signal intensity distributions. Higher signal intensities could be observed within the

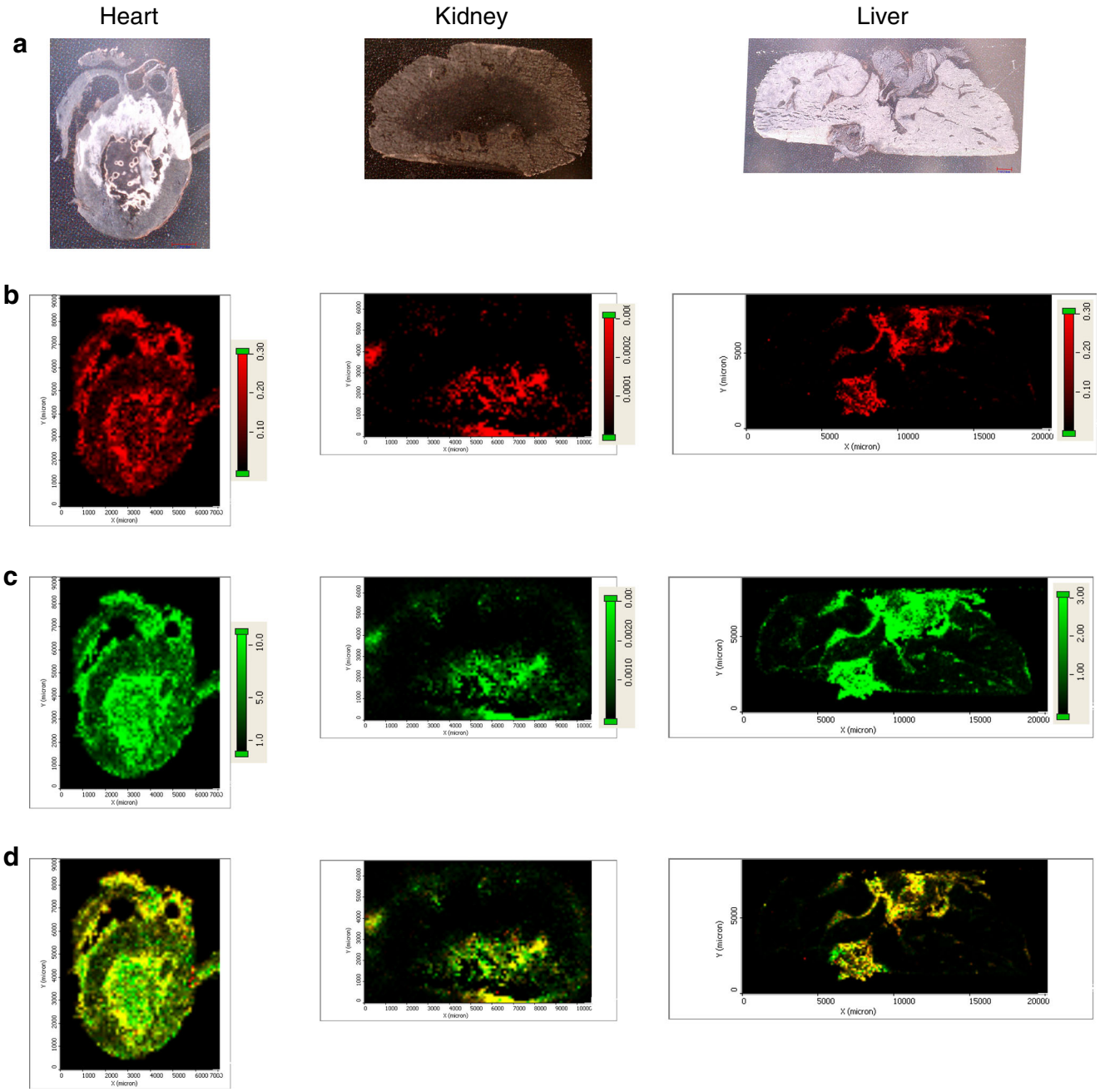

Fig. 3 Distribution of Gadovist™ [Gd (BT-DO3A)+H]$^+$, the free chelate [(BT-DO3A)+H]$^+$, and the combination of both in distinct mouse tissue sections by MALDI-MSI. **a** Optical pictures of mouse heart, kidney, and liver tissue sections before MALDI matrix application. **b** MALDI-MSI image of *m/z* 606.141 ([Gd (BT-DO3A)+H]$^+$) normalized to *m/z* 273.039 ([2 DHB - 2 H_2O+H]$^+$). **c** MALDI-MSI image of *m/z* 451.240 ([(BT-DO3A)+H]$^+$) normalized to *m/z* 273.039. **d** Combination of both

ventricles. As the heart is well supplied with blood, these results were expected in case of an extracellular CA that circles the blood system. Moreover, this GBCA was administered directly into the heart. In respect to the kidney, the analyte [Gd (BT-DO3A)+H]$^+$ was mainly located in the renal pelvis and within the cortex that is imposed by interlobular and arcuate arteries and veins. The liver tissue section also showed signals of [Gd (BT-DO3A)+H]$^+$ in specified areas of the tissue. As MALDI-MSI offers the detection of non-Gd-containing molecules, we also investigated the distribution of the free chelate [(BT-DO3A)+H]$^+$ (Fig. 3c). Surprisingly, the detection of the free chelate ([(BT-DO3A)+H]$^+$) showed higher intensities in comparison to the Gd-containing [Gd (BT-DO3A)+H]$^+$ (Fig. 3b). This is in agreement with our spot MALDI and HPLC-MS analyses, where the non-Gd species also

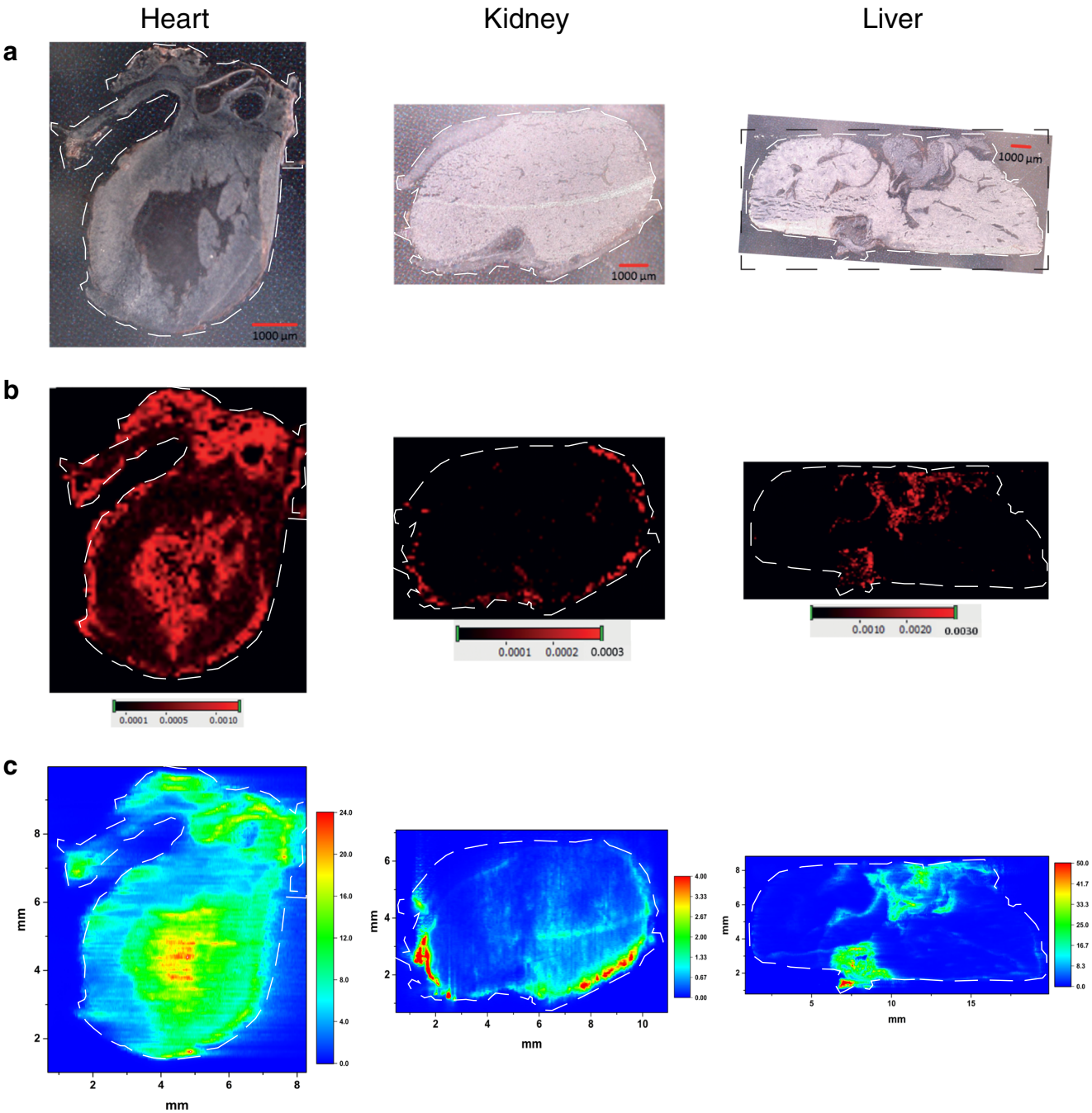

Fig. 4 Gadovist™ imaging in mouse tissue sections. **a** Optical image of a mouse heart, kidney, and liver tissue sections. **b** Corresponding MALDI-MSI analyses of *m/z* 606.141 ($[Gd (BT-DO3A)+H]^+$) normalized to DHB (*m/z* 273.039). **c** Corresponding LA-ICP-MSI analyses showing the distribution of $^{158}Gd^+$ normalized to $^{165}Ho^+$ of the printed Ho ink

showed a higher intensity from commercially available GBCA formulations. Generally, the free chelate collocated well with Gadovist™ in all three mouse organs (Fig. 3d). No Gadovist™ or free chelate was detected in brain thin sections by MALDI-MSI at any time point. Control tissue sections (non-dosed tissues) did not exhibit any signals of $[Gd (BT-DO3A)+H]^+$ or $[(BT-DO3A)+H]^+$ or related species.

LA-ICP-MS imaging

As gadolinium as metal is easily accessible via ICP-MS, we performed LA-ICP-MSI analyses of Gadovist™ in the thin sections of mouse organs. MALDI-MSI does not consume the samples and the MALDI process does not interfere with LA-ICP-MSI; thus, samples obtained after MALDI-MSI were directly assessed with LA-ICP-MSI. The DHB matrix applied

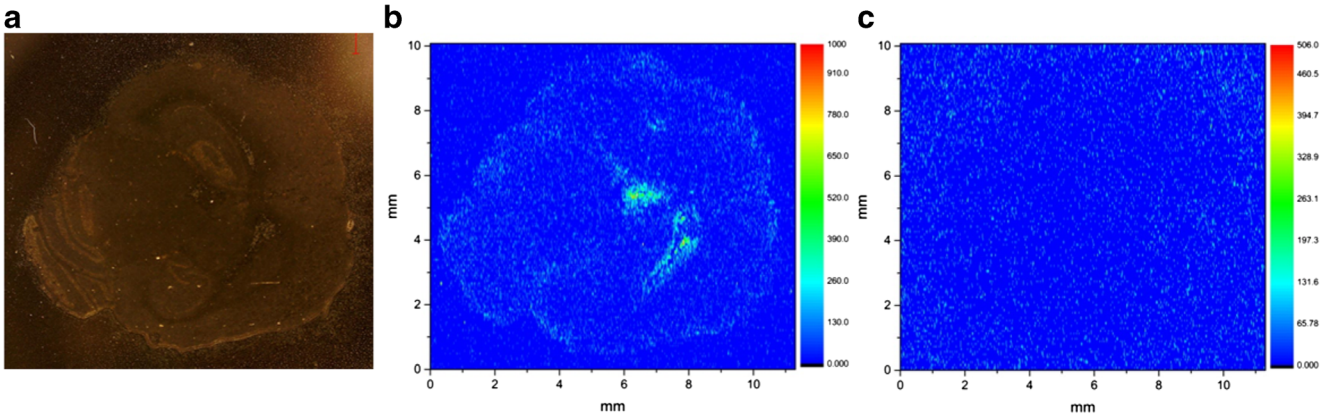

Fig. 5 Gd imaging in a mouse brain tissue section after administration of Gadovist™ by LA-ICP-MSI. **a** Optical image. **b** Distribution of $^{158}Gd^{+}$ normalized to $^{165}Ho^{+}$ from the printed Ho standard. **c** Distribution of $^{153}Eu^{+}$ normalized to $^{165}Ho^{+}$ from the printed Ho standard

in the MALDI-MSI process also did not interfere with the ICP measurements, as no significant signals stemming from rare earth elements were detected from control samples. Initially, we performed LA-ICP-MSI analyses without the application of an internal standard (IS) and detected a drift in signal intensities from the beginning to the end of the experiment (see ESM Fig. S5). Although this is not very pronounced in this case, we have experienced much larger drifts previously. As already known, the ablation process is influenced by the sample matrix and instrumental drifts resulting in an overall loss of sensitivity over time in an analysis [12, 13]. In consequence, the analyses have to be normalized. Initially, elements that should be homogeneously distributed in the tissue sections were selected as ISs. This should account for sodium (^{23}Na) and sulfur (^{34}S). Sodium was ubiquitously represented, and the signal intensity distribution of ^{23}Na was homogeneous over the whole analyzed area. The sulfur isotope ^{34}S represented a homogeneous distribution within the tissue section and less signal intensity in the surrounding area (see ESM Fig. S6). Nevertheless, using these elements has drawbacks. These elements might be less sensitive to instrumental fluctuations in comparison to the analyte ions. Moreover, they have a significant different mass and/or ionization potential. In addition, these elements are not always homogeneously distributed due to differences in tissue water content [14].

Alternatively, we sputtered gold on top of the thin sections after MALDI-MSI to supply a homogeneous gold layer that could act as an IS [15]. Unfortunately, the gold did not show a homogeneous distribution, but resembled the tissue structure and was therefore not suited for normalization (see ESM Fig. S7). Therefore, we decided to print a metal-spiked ink as matrix-adapted standard onto the tissue section after MALDI-MSI [9, 16–18]. Although the Ho distribution were not perfectly homogeneous over the printed area and kidney and liver tissue sections showed lower ^{165}Ho signal intensities in the surroundings of the tissue sections, on the tissue, a rather homogeneous layer of ^{165}Ho was found (see ESM Fig. S8). The inhomogeneities of the printed Ho ink on the tissue appear to be caused by an inhomogeneous height of the thin sections or the different abilities of different tissue areas to adsorb the ink, which affects the deposition of the ink on the surface. Thus, the use of IS printing appears to be not ideal, but currently, it is the most suited approach to normalize LA-ICP-MSI analyses.

Using LA-ICP-MSI, we were able to obtain distributions of the $^{158}Gd^{+}$ signals in all mouse organs. Figure 4c shows the distribution of Gadovist™ in mouse heart, kidney, and liver as assessed by LA-ICP-MSI. The results of the Gadovist™ distributions obtained by MALDI-MSI (Fig. 4b) were so confirmed by LA-ICP-MSI.

Synergies of MALDI-MSI and LA-ICP-MSI

The synergy of elemental MS, such as (LA-)ICP-MS and (bio) molecular mass spectrometry (e.g. MALDI-MS), has already been discussed in general previously [19]. The objective of this study was to investigate the synergy of MALDI- and LA-ICP-MSI for the analysis of GBCAs using Gadovist™. A comparison of Gadovist™ distributions obtained by MALDI-MSI and LA-ICP-MSI is shown in Fig. 4. The results of both, molecular and elemental MSI, were in good agreement. Less intense signals of the compounds could be detected within the tissue sections by MALDI-MSI. It should be noted that during MALDI matrix application, the solvent serves to extract a portion of the analytes from the tissue, while in LA-ICP-MSI, the whole sample material is ablated, which then yields signals from the whole thin section. Furthermore, MALDI-MSI suffers from differences in ionization efficiency due to variations in biological environment and molecular structure, which makes the selection and application of ISs very challenging [11]. In contrary, LA-ICP-MS offers highly sensitive imaging of gadolinium quasi-independently of the original species and sample matrix. Thus, it can yield pivotal information where the limits of detection of MALDI-MSI are not met to detect the analytes. With MALDI-MSI, we were not able to detect the Gadovist™ in the thin section of mouse brains, while in LA-ICP-MS clearly Gd signals were obtained (Fig. 5).

Europium was not detected in this case, strongly suggesting that the detected Gd must stem from the administered Gadovist™.

On the other hand, MALDI-MSI as molecular MS method is in advance over LA-ICP-MSI in respect to information regarding the molecular form or structure of the analyte. It also offers the ability to detect non-metal-containing species, like the free chelate (BT-DO3A). This even showed higher signal intensities compared to the Gd-containing species in MALDI-MSI. While in the current work, no degradation products of Gadovist™ or transmetalation products could be detected, this aspect might be of more importance in the future to monitor biotransformation products of other CAs that are not mainly cleared by filtration.

Summary

Mass spectrometry imaging techniques, e.g., MALDI- and LA-ICP-MSI, turned out to be a powerful tool in the analysis of biodistribution of different pharmaceuticals in a variety of tissues. This work provided an important contribution in parallel application of MALDI- and LA-ICP-MSI to metal-containing GBCAs. As more and more secondary effects related to these agents appeared in recent years, further investigations to study the distribution and accumulation of Gd species in the organism could yield important insights into the fates and distributions of these species. Furthermore, quantification strategies related to MRI CAs should be taken forward regarding both techniques, MALDI- as well as LA-ICP-MSI. LA-ICP-MSI is more straightforward in this context. However, further more extensive steps are necessary and need to be validated (e.g. use of matrix-matched standards or isotopic dilution) before quantification of GBCAs by LA-ICP-MSI can be performed. In terms of MALDI-MSI, it appears much more challenging to provide consistent quantitative data for these GBCAs. Nevertheless, the application of quantitative MALDI has been demonstrated in a number of studies [8, 11, 20–27]. To perform quantitative MSI, an appropriate IS should at first be found for these GBCAs, which is then homogeneously applied to the tissue surface.

In conclusion, each technique namely MALDI- and LA-ICP-MSI as well as MRI has its individual benefits. Only the combination of these methods can solve analytical problems of GBCA investigations. In future, the collective application of these techniques could provide new insights, in particular for the development of more specific CAs.

Compliance with ethical standards

Conflict of interest The authors declare that they have no conflict of interest.

Ethical approval All procedures were approved by the guidelines and regulations of the Federation of Laboratory Animal Science Associations (FELASA) and the local guidelines and provisions for implementation of the Animal Welfare Act. All applicable international, national, and/or institutional guidelines for the care and use of animals were followed.

References

1. Aime S, Dastru W, Crich SG, Gianolio E, Mainero V. Innovative magnetic resonance imaging diagnostic agents based on paramagnetic Gd (III) complexes. Biopolymers. 2002;66(6):419–28. https://doi.org/10.1002/bip.10357.
2. Yan GP, Robinson L, Hogg P. Magnetic resonance imaging contrast agents: overview and perspectives. Radiography. 2007;13:e5–e19.
3. Baranyai Z, Palinkas Z, Uggeri F, Maiocchi A, Aime S, Brucher E. Dissociation kinetics of open-chain and macrocyclic gadolinium (III)-aminopolycarboxylate complexes related to magnetic resonance imaging: catalytic effect of endogenous ligands. Chemistry. 2012;18(51):16426–35. https://doi.org/10.1002/chem.201202930.
4. Kanal E. Gadolinium based contrast agents (GBCA): safety overview after 3 decades of clinical experience. Magn Reson Imaging. 2016;34(10):1341–5. https://doi.org/10.1016/j.mri.2016.08.017.
5. Aime S, Caravan P. Biodistribution of gadolinium-based contrast agents, including gadolinium deposition. J Magn Reson Imaging. 2009;30(6):1259–67. https://doi.org/10.1002/jmri.21969.
6. Kamaly N, Pugh JA, Kalber TL, Bunch J, Miller AD, McLeod CW, et al. Imaging of gadolinium spatial distribution in tumor tissue by laser ablation inductively coupled plasma mass spectrometry. Mol Imaging Biol. 2010;12(4):361–6. https://doi.org/10.1007/s11307-009-0282-4.
7. Lingott J, Lindner U, Telgmann L, Esteban-Fernandez D, Jakubowski N, Panne U. Gadolinium-uptake by aquatic and terrestrial organisms-distribution determined by laser ablation inductively coupled plasma mass spectrometry. Environ Sci Process Impacts. 2016;18(2):200–7. https://doi.org/10.1039/c5em00533g.
8. Aichler M, Huber K, Schilling F, Lohofer F, Kosanke K, Meier R, et al. Spatially resolved quantification of gadolinium (III)-based magnetic resonance agents in tissue by MALDI imaging mass spectrometry after in vivo MRI. Angew Chem Int Ed Engl. 2015;54(14):4279–83. https://doi.org/10.1002/anie.201410555.
9. Moraleja I, Esteban-Fernandez D, Lazaro A, Humanes B, Neumann B, Tejedor A, et al. Printing metal-spiked inks for LA-ICP-MS bioimaging internal standardization: comparison of the different nephrotoxic behavior of cisplatin, carboplatin, and oxaliplatin. Anal Bioanal Chem. 2016;408(9):2309–18. https://doi.org/10.1007/s00216-016-9327-0.
10. Scharlach C, Muller L, Wagner S, Kobayashi Y, Kratz H, Ebert M, et al. LA-ICP-MS allows quantitative microscopy of europium-doped iron oxide nanoparticles and is a possible alternative to ambiguous Prussian blue iron staining. J Biomed Nanotechnol. 2016;12(5):1001–10.
11. Groseclose MR, Castellino S. A mimetic tissue model for the quantification of drug distributions by MALDI imaging mass spectrometry. Anal Chem. 2013;85(21):10099–106. https://doi.org/10.1021/ac400892z.
12. Becker JS, Becker JS. Imaging of metals, metalloids, and non-metals by laser ablation inductively coupled plasma mass spectrometry (LA-ICP-MS) in biological tissues. Methods Mol Biol. 2010;656:51–82. https://doi.org/10.1007/978-1-60761-746-4_3.
13. Frick DA, Günther D. Fundamental studies on the ablation behaviour of carbon in LA-ICP-MS with respect to the suitability as internal standard. J Anal At Spectrom. 2012;27(8):1294–303.
14. Austin C, Fryer F, Lear J, Bishop D, Hare D, Rawling T, et al. Factors affecting internal standard selection for quantitative

elemental bio-imaging of soft tissues by LA-ICP-MS. J Anal At Spectrom. 2011;26(7):1494–501.
15. Konz I, Fernandez B, Fernandez ML, Pereiro R, Gonzalez H, Alvarez L, et al. Gold internal standard correction for elemental imaging of soft tissue sections by LA-ICP-MS: element distribution in eye microstructures. Anal Bioanal Chem. 2013;405(10):3091–6. https://doi.org/10.1007/s00216-013-6778-4.
16. Hoesl S, Neumann B, Techritz S, Linscheid M, Theuring F, Scheler C, et al. Development of a calibration and standardization procedure for LA-ICP-MS using a conventional ink-jet printer for quantification of proteins in electro- and Western-blot assays. J Anal At Spectrom. 2014;29(7):1282–91.
17. Bellis DJ, Santamaria-Fernandez R. Ink jet patterns as model samples for the development of LA-ICP-SFMS methodology for mapping of elemental distribution with reference to biological samples. J Anal At Spectrom. 2010;25(7):957–63.
18. Hoesl S, Neumann B, Techritz S, Sauter G, Simon R, Schlüter H, et al. Internal standardization of LA-ICP-MS immuno imaging via printing of universal metal spiked inks onto tissue sections. J Anal At Spectrom. 2016;31(3):801–8.
19. Becker JS, Jakubowski N. The synergy of elemental and biomolecular mass spectrometry: new analytical strategies in life sciences. Chem Soc Rev. 2009;38(7):1969–83. https://doi.org/10.1039/b618635c.
20. Buck A, Halbritter S, Spath C, Feuchtinger A, Aichler M, Zitzelsberger H, et al. Distribution and quantification of irinotecan and its active metabolite SN-38 in colon cancer murine model systems using MALDI MSI. Anal Bioanal Chem. 2015;407(8):2107–16. https://doi.org/10.1007/s00216-014-8237-2.
21. Chumbley CW, Reyzer ML, Allen JL, Marriner GA, Via LE, Barry CE 3rd, et al. Absolute quantitative MALDI imaging mass spectrometry: a case of rifampicin in liver tissues. Anal Chem. 2016;88(4):2392–8. https://doi.org/10.1021/acs.analchem.5b04409.
22. Lagarrigue M, Lavigne R, Tabet E, Genet V, Thome JP, Rondel K, et al. Localization and in situ absolute quantification of chlordecone in the mouse liver by MALDI imaging. Anal Chem. 2014;86(12):5775–83. https://doi.org/10.1021/ac500313s.
23. Landgraf RR, Garrett TJ, Conaway MC, Calcutt NA, Stacpoole PW, Yost RA. Considerations for quantification of lipids in nerve tissue using matrix-assisted laser desorption/ionization mass spectrometric imaging. Rapid Commun Mass Spectrom. 2011;25(20):3178–84. https://doi.org/10.1002/rcm.5189.
24. Marsching C, Jennemann R, Heilig R, Grone HJ, Hopf C, Sandhoff R. Quantitative imaging mass spectrometry of renal sulfatides: validation by classical mass spectrometric methods. J Lipid Res. 2014;55(11):2343–53. https://doi.org/10.1194/jlr.M051821.
25. Nakanishi T, Takai S, Jin D, Takubo T. Quantification of candesartan in mouse plasma by MALDI-TOFMS and in tissue sections by MALDI-imaging using the stable-isotope dilution technique. Mass Spectrom (Tokyo). 2013;2(1):A0021. https://doi.org/10.5702/massspectrometry.A0021.
26. Pirman DA, Reich RF, Kiss A, Heeren RM, Yost RA. Quantitative MALDI tandem mass spectrometric imaging of cocaine from brain tissue with a deuterated internal standard. Anal Chem. 2013;85(2):1081–9. https://doi.org/10.1021/ac302960j.
27. Schulz S, Gerhardt D, Meyer B, Seegel M, Schubach B, Hopf C, et al. DMSO-enhanced MALDI MS imaging with normalization against a deuterated standard for relative quantification of dasatinib in serial mouse pharmacology studies. Anal Bioanal Chem. 2013;405(29):9467–76. https://doi.org/10.1007/s00216-013-7393-0.